Stability of two- and three-dimensional excitonic complexes

J. Usukura
Graduate School of Science and Technology, Niigata University, Niigata 950-2181, Japan

Y. Suzuki
Department of Physics, Niigata University, Niigata 950-2181, Japan

K. Varga*
Institute for Physical and Chemical Research (RIKEN), Wako, Saitama 351-0198, Japan
and Physics Division, Argonne National Laboratory, 9700 South Cass Avenue, Argonne, Illinois 60439
(Received 5 October 1998)

The binding energies and other properties of the excitonic complexes (bound systems of electrons and holes) in two and three dimensions (2D and 3D) are calculated by a precise variational method. The mass ratios for the limit of the stability of $X_3^+(eehh)$ are determined in both 2D and 3D cases. Two excited states of the biexciton are found to remain bound for any mass ratio. [S0163-1829(99)01608-2]

I. INTRODUCTION

The excitonic complexes (or molecules) including the charged excitons have considerable importance in the development of semiconductor physics and spectroscopy. In particular, the biexciton has been a subject of intensive experimental[1–3] and theoretical[4–10] investigation. The constituents of these systems are electrons and holes with masses m_e^* and m_h^*, interacting via Coulomb interactions. Here m_e^* and m_h^* are ''effective masses.'' The properties and structure of these systems significantly change with the mass ratio $\sigma=m_e^*/m_h^*$, and by approaching the two limiting cases, hydrogenic ($\sigma=0$) and positronium ($\sigma=1$) limits, one arrives at two completely different worlds.

There are several discrepancies between theory and experiment. The most striking one is the difference between the experimentally estimated and theoretically predicted ratio of the binding energies of the biexciton and the exciton. There are several suggestions for additional binding mechanisms to resolve these problems, for example the stronger binding might be due to some localization or confinement effect.[11] The aim of the present paper is to investigate a clean model case: to pinpoint the energies of the excitonic complexes interacting via pure Coulomb forces in two and three dimensions (2D and 3D) and to show how much of the binding energy has to be brought by other mechanisms to reconcile the experiment with theory.

In the hydrogenic limit, several systems, e.g., $H^-(eeh)$, $H_2{}^+(ehh)$, $H_2(eehh)$, $H_3{}^+(eehhh)$, or $H_4{}^+(eeehhhh)$, etc. form bound states. By changing the mass ratio and approaching the positronium limit, the systems containing not more than four particles remain stable, but there is no proof of existence for systems consisting of more than four particles with equal mass. It is therefore intriguing to ask a question: What is the mass ratio where the stability is lost? If experiments show the existence of a stable system beyond the predicted stability limit of pure Coulomb interactions, it is a clear signature of other binding mechanisms which are not accounted for in the present model.

Another interest is the information on the sizes of these systems. Approaching the stability border, these species are very loosely bound and therefore their sizes (root-mean-square radii, distances between particles) substantially increase. With the advent of nanotechnology it has become possible to fabricate small semiconductor structures where the thickness of a quantum well is comparable to the size of an electron-hole system. The root-mean-square radii and the distances between the particles of these excitonic complexes change with the mass ratio. We will point out that the electron-hole distances can be quite different in different materials.

Most of theoretical approaches are variational, utilizing different forms of basis functions.[4–7] Some calculations attempt to reduce the few-particle Hamiltonian to that of a smaller system with fewer degrees of freedom.

The hydrogenic and positronium limits have been very extensively studied in atomic and molecular physics, and the theoretical and experimental results are in perfect agreement. It is interesting and useful to borrow the sophisticated technique of atomic and molecular physicists to study these systems, even though we are aware that the 3D excitonic complexes (with pure Coulomb interaction) are only models of the real experimental situation. While most of the previous calculations are based on several simplifying assumptions, e.g., the neglect of exchange interactions or electronic correlations, the approach we present here is free from any such approximations and the result can be considered as virtually exact. As will be seen later, our calculation reproduces the energies of the two limiting cases as it should.

To solve the Schrödinger equation of the Coulombic few-body problem, we use the stochastic variational method with correlated Gaussian basis.[12–15] The correlated Gaussian functions serve as a quite suitable basis for accurate calculations of few-electron atoms and small molecules. They have been widely used in atomic and molecular physics.[16–18] The applications include the analogous systems of excitonic complexes such as H_2, $H_2{}^+$, or the positronium molecule (Ps_2) and the binding energies are calculated up to 8–10 digits of

accuracy. The adequate choice of the nonlinear parameters of the correlated Gaussians is an essential requirement. To select the most appropriate ones, the stochastic variational method has been used. The stochastic variational method tests the quality of the basis states by a random trial and error procedure. This method is proved to be quite successful in solving various few-particle problems.[19]

The plan of this paper is as follows. The Introduction is followed by Sec. II, where we outline the problem and the method of solution. In Sec. III we present the results for 3D and 2D systems. The results are discussed in Sec. IV.

II. MODEL OF EXCITONIC COMPLEXES AND METHODS OF CALCULATION

The general Hamiltonian of the excitonic complexes, the systems of N_e electrons in positions $\mathbf{r}_1,\ldots,\mathbf{r}_{N_e}$ and N_h holes in positions $\mathbf{r}_{N_e+1},\ldots,\mathbf{r}_N$ $(N=N_e+N_h)$, can be written as

$$H=\sum_{i=1}^{N_e}\frac{\mathbf{p}_i^2}{2m_e^*}+\sum_{i=N_e+1}^{N}\frac{\mathbf{p}_i^2}{2m_h^*}+\sum_{i<j}^{N_e}\frac{e^2}{\epsilon|\mathbf{r}_i-\mathbf{r}_j|}-\sum_{i=1}^{N_e}\sum_{j=N_e+1}^{N}\frac{e^2}{\epsilon|\mathbf{r}_i-\mathbf{r}_j|}+\sum_{N_e<i<j}^{N}\frac{e^2}{\epsilon|\mathbf{r}_i-\mathbf{r}_j|}, \quad (1)$$

where ϵ is the dielectric constant of the material. The vectors are either 3D or, if the well thickness is ignored, they are 2D. The length and the energy are measured in excitonic units with the ''Bohr radius'' $a_x=\hbar^2\epsilon/(m_e^*e^2)$ and the ''Rydberg energy'' $R_x=e^2/(2\epsilon a_x)=e^4m_e^*/(2\hbar^2\epsilon^2)$. In these units the Hamiltonian (1) depends on only the mass ratio σ. In the case where m_e^* is equal to the free electron mass and ϵ is equal to unity, the excitonic units reduce to the usual atomic units (to be exact, the unit of energy reduces to one-half of the energy of the atomic unit). In general we are interested in calculating the intrinsic energy which has no contribution from the center-of-mass motion. To this end it is convenient to introduce an appropriate set of relative coordinates $\{\mathbf{x}_1,\ldots,\mathbf{x}_{N-1}\}$ and the center-of-mass coordinate $\mathbf{x}_N=(\Sigma_{i=1}^{N_e}m_e^*\mathbf{r}_i+\Sigma_{i=N_e+1}^{N}m_h^*\mathbf{r}_i)/(N_em_e^*+N_hm_h^*)$.

To solve the eigenvalue problem of the above Hamiltonian, we assume the variational trial function Ψ to be given as combinations of correlated Gaussians:

$$\Psi=\sum_A C_A\mathcal{A}\{G_A(\mathbf{r})\chi(1,\ldots,N)\}. \quad (2)$$

Here $\mathcal{A}$ is the operator which produces a properly antisymmetrized wave function for the electrons and the holes, respectively. The function $\chi(1,\ldots,N)$ is the spin function for the electrons and the holes. Though the Hamiltonian (1) is spin-independent, the symmetry property of the spin function is an important ingredient in determining the stability of the system because it affects the spatial symmetry of the system. The correlated Gaussian is defined by

$$G_A(\mathbf{r})=\exp\{-\tfrac{1}{2}\tilde{\mathbf{r}}A\mathbf{r}\}=\exp\left\{-\frac{1}{2}\sum_{i=1}^{N}\sum_{j=1}^{N}A_{ij}\mathbf{r}_i\cdot\mathbf{r}_j\right\}, \quad (3)$$

where $\tilde{\mathbf{r}}$ stands for a row vector $(\mathbf{r}_1,\mathbf{r}_2,\ldots,\mathbf{r}_N)$ whose ith element is $\mathbf{r}_i$. The elements of a positive-definite, symmetric matrix $A=(A_{ij})$ are variational parameters which characterize the basis function.

The function (3) contains the center-of-mass coordinate dependence. The separation of the center-of-mass motion from Eq. (3) can be easily done by imposing the following constraints on A:[15]

$$\sum_{j=1}^{N}\sum_{k=1}^{N}A_{jk}U_{ki}^{-1}=0\quad(i=1,\ldots,N-1),\qquad \sum_{j=1}^{N}\sum_{k=1}^{N}A_{jk}=c, \quad (4)$$

where c is an arbitrary, positive constant common to each basis function. Here U is the matrix which connects the single-particle coordinates $\mathbf{r}$ and the relative and center-of-mass coordinates $\mathbf{x}=\{\mathbf{x}_1,\mathbf{x}_2,\ldots,\mathbf{x}_N\}$:

$$\mathbf{x}=U\mathbf{r},\quad \mathbf{r}=U^{-1}\mathbf{x}. \quad (5)$$

It is easy to see that under the condition (4) the center-of-mass motion contained in Eq. (3) separates from the intrinsic motion depending on only the relative coordinates and takes the form $\exp(-c\mathbf{x}_N^2/2)$, which is common to all the basis functions. This separability enables one to calculate the matrix element of the intrinsic Hamiltonian $H_{\rm int}=H-T_{\rm cm}$, with $T_{\rm cm}$ being the center-of-mass kinetic energy.

The correlated Gaussian (3) is rotationally invariant and describes the motion with zero total orbital angular momentum for the 3D case or with vanishing z component of the total orbital angular momentum for the 2D case when the motion is on the xy plane. This assumption is acceptable because we are interested in the ground state which is expected to have such symmetry.

For the systems with nonzero σ value we have used the trial function (2). The matrix A, containing $N(N-1)/2$ free parameters, describes the correlated motion between the particles. In the hydrogenic limit $(\sigma=0)$, however, the holes are infinitely heavy so that they can be placed at some fixed spatial points. The center-of-mass of the holes is conveniently taken as the coordinate origin. The kinetic energy of the holes is suppressed and thus the position coordinates of the holes can be treated as just c numbers. Thus we only need to consider the motion of the electrons that move in the Coulomb potential field created by the holes. The geometrical arrangement of the holes is assumed to form, e.g., an equilateral triangle for the system with three holes. The length of the triangle is varied to reach an energy minimum. In order to represent several ''peaks'' of the density distribution of the electrons when the holes are well separated and the electrons are on ''atomic orbits'' around them, we extend the correlated Gaussian of Eq. (3) as follows:

$$G_{A\mathbf{s}}(\mathbf{r})=\exp\{-\tfrac{1}{2}\tilde{\mathbf{r}}A\mathbf{r}+\tilde{\mathbf{s}}\mathbf{r}\}. \quad (6)$$

Here $\mathbf{r}=\{\mathbf{r}_1,\ldots,\mathbf{r}_{N_e}\}$ stands for the positions of the electrons only and the ''generator'' coordinates $\mathbf{s}=\{\mathbf{s}_1,\ldots,\mathbf{s}_{N_e}\}$ are variational parameters which are chosen in conformity with $\mathbf{r}$.

TABLE I. Energies and binding energies of the 2D and 3D excitonic complexes in the hydrogenic ($\sigma=0$) and positronium ($\sigma=1$) limits. σ is the mass ratio m_e^*/m_h^* of the electron and the hole. The asterisk refers to the state which is found to be unbound. The unit of energy is the excitonic Rydberg.

System	2D				3D			
	$E(\sigma=0)$	$E(\sigma=1)$	$B(\sigma=0)$	$B(\sigma=1)$	$E(\sigma=0)$	$E(\sigma=1)$	$B(\sigma=0)$	$B(\sigma=1)$
eh	−4.000	−2.000	4.000	2.000	−1.000	−0.500	1.000	0.500
eeh	−4.480	−2.242	0.480	0.242	−1.055	−0.524	0.055	0.024
ehh	−5.639	−2.242	1.639	0.242	−1.204	−0.524	0.204	0.024
$eehh$	−10.66	−4.385	2.660	0.385	−2.349	−1.032	0.348	0.032
$eeehh$	*	*	*	*	*	*	*	*
$eehhh$	−13.65	*	2.992	*	−2.687	*	0.338	*

The above basis function (6) includes $N_e(N_e+1)/2+dN_e$ $(d=2,3)$ parameters to be optimized. By choosing $\mathbf{s}=0$, the trial function has its maximum at the origin and this limit is quite suitable around $\sigma=1$, when the particles with nearly equal mass are moving equally fast. At the hydrogenic limit, when the motion of the heavy particles is very slow compared to the light ones, the density distribution has several peaks around the attractive centers, and to represent these configurations we need to shift the maximum of the trial functions out of the origin by choosing $\mathbf{s}$ appropriately.

One of the advantages of the correlated Gaussians is that their matrix elements are readily available analytically (see, e.g., Refs. 12 and 19). The most adequate parameters are selected by the stochastic variational method. The basic idea is to generate several sets of parameters randomly and choose the one which gives the lowest energy. The details of the method are given elsewhere.[12,19] There are many examples[12,15,19] that demonstrate the high accuracy of calculations attained in the stochastic variational approach with the correlated Gaussian basis.

All possible spin functions are tested and the one giving the lowest energy is chosen in what follows. For example, for the system including two electrons (or holes) they are taken to be in a spin-singlet state, and for the case with three electrons (or holes) the most favorable spin function is found to be a state with mixed symmetry, i.e.,

$$\chi(1,2,3)=\{\alpha(1)\beta(2)-\beta(1)\alpha(2)\}\alpha(3). \tag{7}$$

III. RESULTS

The results of our calculation for the energies $E(\sigma)$ and the binding energies $B(\sigma)$ at the two limiting cases are collected in Table I for 2D and 3D systems. The energies are in perfect agreement with other theoretical results in 3D for H_2^+, H^-, $H_2(\sigma=0)$ and Ps^-, Ps_2 $(\sigma=1)$. The positronium molecule Ps_2 has not yet been found experimentally. The total energies of the 2D and 3D excitonic complexes are summarized in Figs. 1 and 2 as a function of σ. In the figures the relevant threshold energies are also drawn by dashed curves as a function of σ to get information on the binding energies. In both 2D and 3D cases the charged excitons, $X^-(eeh)$ and $X_2^+(ehh)$, and the biexciton $X_2(eehh)$ are all bound for all σ values. The charged biexciton $(eeehh)$ is unbound for all values of σ but we have found that $X_3^+(eehhh)$, a semiconductor analog of H_3^+, is bound for $\sigma<\sigma_{cr}$. The critical value σ_{cr} for its stability is given by the point where the energy curves of X_2 and X_3^+ merge, and will be discussed later. We see that the binding energy of the 2D system is almost a factor of 10 larger than that of the corresponding 3D system. The binding energy in general decreases by increasing σ from 0 to 1, and this trend is especially dramatic in the case of X_2^+.

A. Three-body systems

Figure 3 compares the binding energies of the three-body excitonic complexes, X^- and X_2^+, with the energies pre-

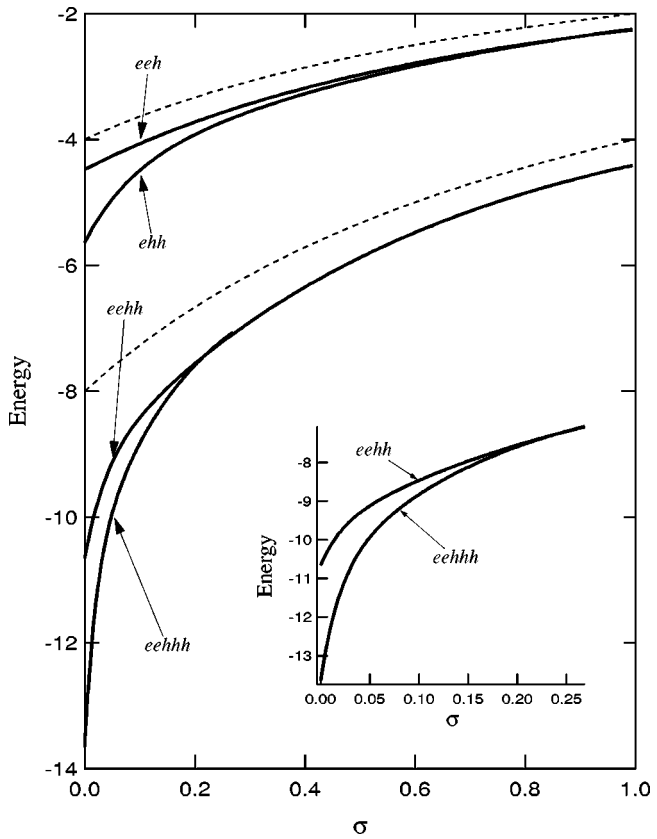

FIG. 1. The total energies of two-dimensional excitonic complexes as a function of the mass ratio of the electron and the hole, $\sigma=m_e^*/m_h^*$. The dashed curves are the threshold energies for the three-body and four-body complexes. The inset is a magnification of energy curves for the four- and five-body complexes at small σ values. The energy is in units of the excitonic Rydberg.

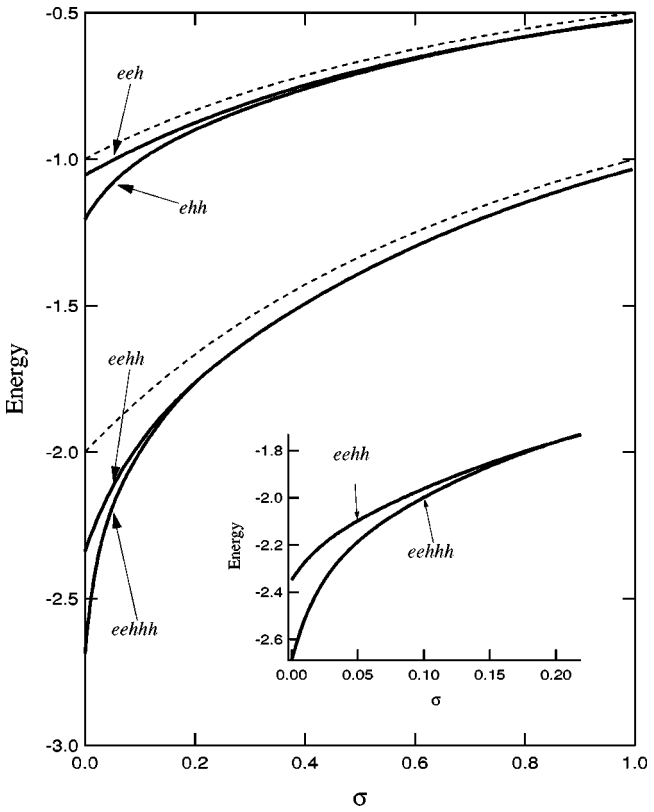

FIG. 2. The total energies of three-dimensional excitonic complexes as a function of the mass ratio of the electron and the hole, $\sigma = m_e^*/m_h^*$. See the caption of Fig. 1.

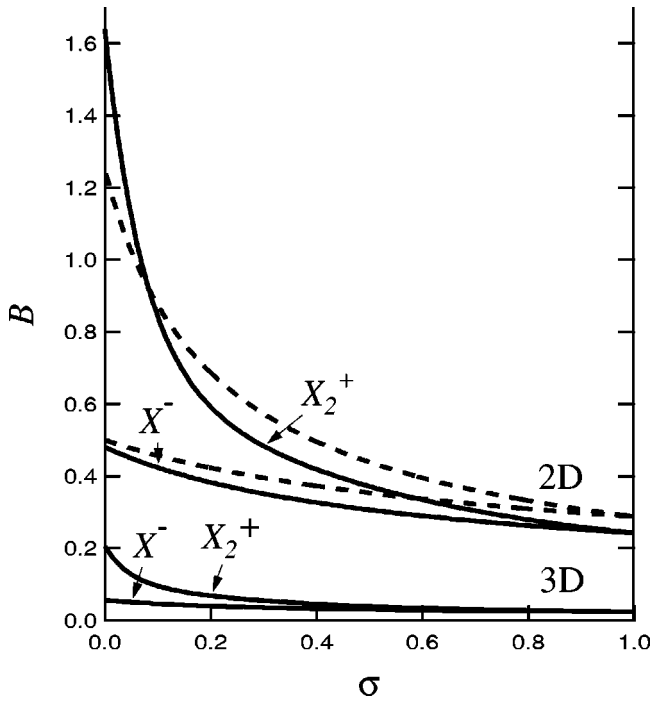

FIG. 3. The binding energies of the charged excitons X^- (eeh) and X_2^+ (ehh) as a function of the mass ratio σ. The dashed curves refer to a linear model calculation of Ref. 21. The energy is in units of the excitonic Rydberg.

dicted by other models.[20] Though the X^- result is in reasonable agreement with the other calculations, there is a noticeable difference in the X_2^+ curve at small σ, which indicates that a linear model[20] is not a realistic approximation. By changing σ (and therefore the binding energy), the average distances between the particles also substantially change. See Table II and Fig. 4. Here $\langle r_{ij}\rangle$ and $\langle r_{ij}^2\rangle$ indicate the expectation values $\langle|\mathbf{r}_i-\mathbf{r}_j|\rangle$ and $\langle(\mathbf{r}_i-\mathbf{r}_j)^2\rangle$, respectively and $\langle\delta(r_{ij})\rangle$ the expectation value $\langle\delta(\mathbf{r}_i-\mathbf{r}_j)\rangle$. The distance between the holes in X_2^+ increases by a factor of four by changing σ from $\sigma=0$ to $\sigma=1$. The equilibrium distance between the two holes in 3D X_2^+ system (H_2^+) is 1.997 Bohr, in excellent agreement with the value (2 Bohr) found in adia-

TABLE II. Properties of the 2D and 3D charged excitons, X^- (eeh) and X_2^+ (ehh), as a function of the mass ratio σ. The excitonic units are used.

	2D				3D			
	$\sigma=0$	$\sigma=0.4$	$\sigma=0.7$	$\sigma=1$	$\sigma=0$	$\sigma=0.4$	$\sigma=0.7$	$\sigma=1$
X^- (eeh)								
$-E$	4.480	3.18	2.627	2.242	1.055	0.746	0.615	0.524
$\langle r_{--}\rangle$	1.40	1.94	2.28	2.59	4.41	6.334	7.497	8.55
$\langle r_{+-}\rangle$	0.86	1.22	1.45	1.68	2.71	3.964	4.756	5.49
$\langle r_{--}^2\rangle$	2.69	5.15	7.04	8.95	25.2	52.12	72.25	93.2
$\langle r_{+-}^2\rangle$	1.27	2.58	3.63	4.71	11.9	26.00	36.87	48.4
$\langle\delta(r_{--})\rangle$	0.11	0.049	0.029	0.020	0.0028	0.00071	0.00033	0.00017
$\langle\delta(r_{+-})\rangle$	1.5	0.78	0.53	0.38	0.16	0.059	0.033	0.021
X_2^+ (ehh)								
$-E$	5.639	3.276	2.656	2.242	1.205	0.759	0.619	0.524
$\langle r_{++}\rangle$	0.518	1.60	2.12	2.59	1.997	5.200	6.856	8.55
$\langle r_{+-}\rangle$	0.470	1.08	2.78	1.68	1.657	3.495	4.485	5.49
$\langle r_{++}^2\rangle$	0.268	3.28	5.92	8.95	3.989	32.93	58.21	93.2
$\langle r_{+-}^2\rangle$	0.298	1.86	3.20	4.71	3.389	18.26	31.01	48.4
$\langle\delta(r_{++})\rangle$	0	0.027	0.025	0.020	0	0.00026	0.00024	0.00017
$\langle\delta(r_{+-})\rangle$	2.08	0.81	0.54	0.38	0.21	0.062	0.034	0.021

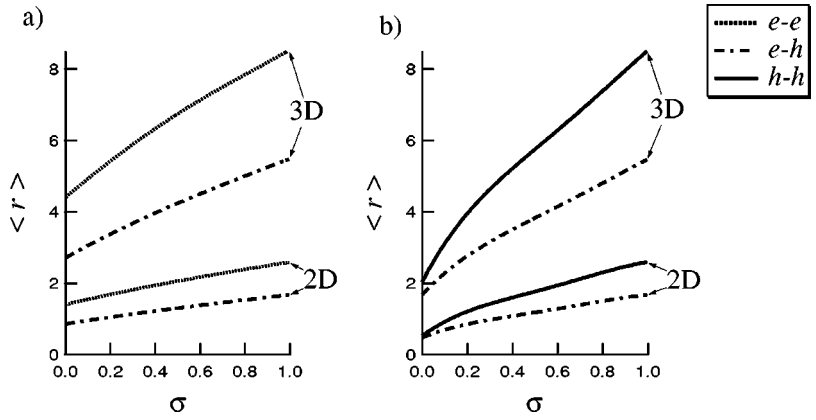

FIG. 4. The average distances of the constituents in the charged excitons as a function of the mass ratio σ. (a) for X^- (eeh) and (b) for X_2^+ (ehh). The length is in units of the excitonic Bohr radius.

batic calculations.[21] Except for the case of the hydrogenic limit, the ratio of the standard deviation of the average distance to the distance itself, $\sqrt{\langle(r-\langle r\rangle)^2\rangle}/\langle r\rangle$, is large, typically around 0.5 for the particles with identical charges and 0.7–0.8 for the particles with opposite charges. This shows that it is not possible to have a geometrical picture of these systems. One cannot interpret these systems as forming a triangle even in the 2D case.

B. Four-body systems

The binding energy decreases by increasing σ from 0 to 1 (see Figs. 1 and 2) and the binding energy of the 2D case is much larger than that of the 3D one. Figure 5 displays the Haynes factor $f_H = B_{X_2}/B_X$, where B_X and B_{X_2} are the binding energies of the exciton and the biexciton, respectively. As mentioned in the Introduction, the Haynes factor estimated experimentally differs from the value of the theoretical calculations. Our calculation shows that the factor f_H decreases from 0.348 at $\sigma=0$ to 0.064 at $\sigma=1$ for the 3D case, while it decreases from 0.665 at $\sigma=0$ to 0.193 at $\sigma=1$ for 2D. Our values for 2D are significantly larger than those of Ref. 6, which gives $f_H=0.564$ at $\sigma=0$ and 0.14 at $\sigma=1$. The Haynes factor predicted in the pure 2D calculation is 0.20 at $\sigma=0.68$ (GaAs), which is in good agreement with the experimental value $f_H \approx 0.2$.[3]

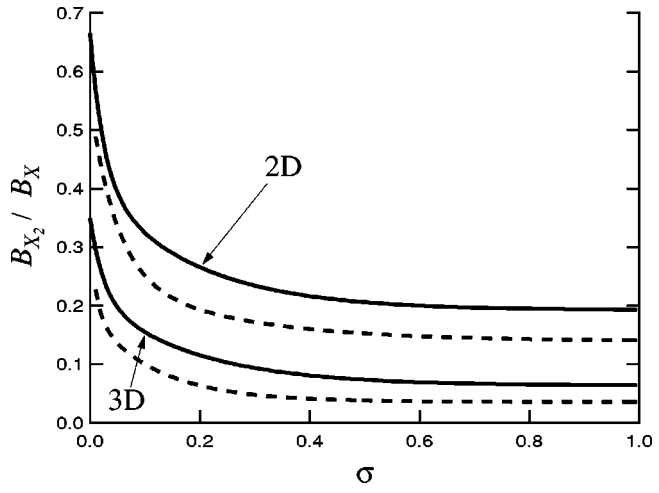

FIG. 5. The binding energy of the biexciton X_2 $(eehh)$ compared to the binding energy of the exciton X as a function of the mass ratio σ. The dashed curves refer to a variational calculation of Ref. 6.

The σ dependence of the average distances between the particles in X_2 is shown in Fig. 6. The expectation value $\langle r\rangle$ (and also $\langle r^2\rangle$) decreases with decreasing σ. The average distances between h-h $(\langle r_{++}\rangle)$ and e-$e$$(\langle r_{--}\rangle)$ are different in the hydrogenic limit $(\sigma=0)$, and gradually tend to the same value at the equal mass end $(\sigma=1)$. Naturally, in order to minimize the Coulomb energy, the distance between the positive and negative charges is expected to be smaller than that between the particles with identical charges. This is what we see in Fig. 6 and Table III, except around $\sigma=0$. Around the hydrogenic limit the average distance between the holes becomes smaller than that between the electron and the hole. This indicates that the binding mechanism has changed. The equilibrium distance between the two infinitely

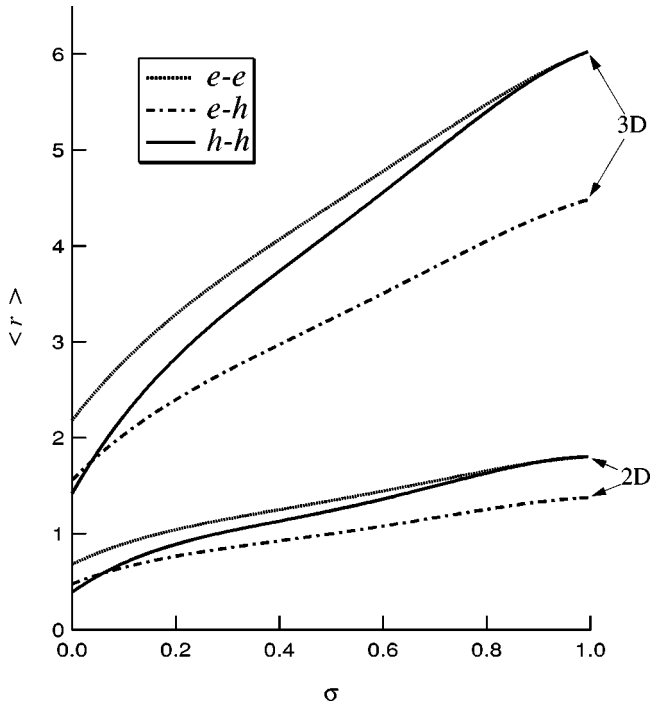

FIG. 6. The average distances of the constituents in the biexciton X_2 $(eehh)$ as a function of the mass ratio σ. The length is in units of the excitonic Bohr radius.

TABLE III. Properties of the 2D and 3D biexcitons X_2 $(eehh)$ as a function of the mass ratio σ. The excitonic units are used.

	2D				3D			
	$\sigma=0$	$\sigma=0.4$	$\sigma=0.7$	$\sigma=1$	$\sigma=0$	$\sigma=0.4$	$\sigma=0.7$	$\sigma=1$
$-E$	10.66	6.335	5.168	4.385	2.349	1.487	1.215	1.032
$\langle r_{--}\rangle$	0.671	1.26	1.55	1.80	2.17	4.08	5.12	6.03
$\langle r_{++}\rangle$	0.371	1.14	1.49	1.80	1.40	3.75	4.97	6.03
$\langle r_{+-}\rangle$	0.467	0.930	1.16	1.38	1.55	2.98	3.77	4.49
$\langle r_{--}^2\rangle$	0.592	2.09	3.19	4.33	5.34	20.7	33.1	46.4
$\langle r_{++}^2\rangle$	0.138	1.69	2.95	4.33	1.97	17.3	31.1	46.4
$\langle r_{+-}^2\rangle$	0.309	1.29	2.05	2.88	3.04	12.4	20.3	29.1
$\langle \delta(r_{--})\rangle$	0.48	0.12	0.071	0.048	0.017	0.0027	0.0013	0.00063
$\langle \delta(r_{++})\rangle$	0	0.074	0.061	0.048	0	0.0013	0.00094	0.00063
$\langle \delta(r_{+-})\rangle$	2.2	0.86	0.57	0.41	0.23	0.065	0.036	0.022

heavy particles ($\sigma=0$) for 3D is found to be 1.40 Bohr, in agreement with the calculated value for H_2.[21]

Our results do not support the basic assumption of Ref. 22, in which it was assumed that the 2D X_2 forms a square where the opposite charges are situated in the opposite vertices of the square. In our work we can evaluate the average distances and the variances of the average distances between the particles without any model assumption. First we point out that, except for the case of heavy positive charges, all the variances of average distances are large, so that no geometrical interpretation can be made in 2D. Second, the distances between the $++$ and $--$ charges are not equal, except for the $\sigma=1$ case, so that they do not form a square. They do not sit on the vertices of a square for $\sigma=1$ either, because $\langle r_{++}\rangle/\langle r_{+-}\rangle \neq \sqrt{2}$.

Table III also shows the probability of finding two particles at the same point in coordinate space.

C. Five-body systems

As mentioned at the beginning of this section, the charged biexciton X_3^+ $(eehhh)$ forms a bound system for small values of σ, while the $(eeehh)$ system is unbound for any values of σ. This is in contradiction with the result of Ref. 20, which relies on a schematic model for these five-body excitonic complexes. In Table IV we tabulate the total energies of X_2 and X_3^+ for various values of σ. The binding energy of X_3^+, $B_{X_3^+}$, is given by $E_{X_2}-E_{X_3^+}$. To determine the critical mass ratio, accurate calculations are needed. We have obtained that $B_{X_3^+}=2.99$ Rydberg at $\sigma=0$ in the 2D case, whereas it decreases to 0.338 Rydberg in the 3D case. The binding energy gets smaller as σ increases. The critical σ value is found to be

$$0.26<\sigma_{\rm cr}<0.27 \ \text{ for 2D}, \qquad 0.22<\sigma_{\rm cr}<0.23 \ \text{ for 3D}. \tag{8}$$

No experimental confirmation has been obtained yet for the existence of the charged biexciton X_3^+.

The structure change of X_3^+, when approaching the border of the stable region, is interesting. Table V lists the properties of X_3^+ as a function of σ. Figure 7 plots the change of the average distances between the particles as a function of σ. It is noted that the *h-h* and *e-h* distances significantly increase with σ approaching the $\sigma_{\rm cr}$ value but the *e-e* distance remains rather stable. This suggests that though the three holes form an equilateral triangle with a length of 1.65 Bohr at $\sigma=0$ (in 3D), one of the holes tends to separate from

TABLE IV. Energies of the 2D and 3D charged biexciton X_3^+ $(eehhh)$, given in units of the excitonic Rydberg, as a function of the mass ratio σ. E_{X_2} and $E_{X_3^+}$ are the total energies of the biexciton and the charged biexciton, respectively, and $B_{X_3^+}=E_{X_2}-E_{X_3^+}$ is the binding energy of the charged biexciton.

2D				3D			
σ	$-E_{X_2}$	$-E_{X_3^+}$	$B_{X_3^+}$	σ	$-E_{X_2}$	$-E_{X_3^+}$	$B_{X_3^+}$
0	10.66	13.65	2.99	0	2.349	2.687	0.338
0.05	9.116	9.936	0.821	0.02	2.199	2.350	0.151
0.10	8.457	8.830	0.373	0.05	2.092	2.187	9.48×10^{-2}
0.15	7.9616	8.1192	0.158	0.10	1.9597	1.999	3.98×10^{-2}
0.20	7.5481	7.5936	4.55×10^{-2}	0.15	1.8530	1.8665	1.35×10^{-2}
0.25	7.191311	7.194725	3.41×10^{-3}	0.20	1.76212	1.76416	2.05×10^{-3}
0.26	7.1252300	7.1261974	9.67×10^{-4}	0.21	1.74534	1.74637	1.02×10^{-3}
0.27	7.0606665	7.0596177	unbound	0.22	1.728977	1.729144	1.67×10^{-4}
				0.23	1.712999	1.712722	unbound

TABLE V. Properties of the 2D and 3D charged biexcitons X_3^+ $(eehhh)$ as a function of the mass ratio σ. The excitonic units are used.

	2D				3D			
	$\sigma=0$	$\sigma=0.05$	$\sigma=0.15$	$\sigma=0.25$	$\sigma=0$	$\sigma=0.05$	$\sigma=0.15$	$\sigma=0.21$
$-E$	13.65	9.936	8.1192	7.194725	2.687	2.187	1.8665	1.74637
$\langle r_{--}\rangle$	0.556	0.881	1.187	1.165	1.986	2.841	3.595	3.584
$\langle r_{++}\rangle$	0.404	0.887	1.487	4.467	1.652	2.929	4.699	9.118
$\langle r_{+-}\rangle$	0.424	0.733	1.103	2.619	1.572	2.392	3.466	5.727
$\langle r_{--}^2\rangle$	0.397	0.999	1.881	1.853	4.517	9.688	16.18	16.29
$\langle r_{++}^2\rangle$	0.163	0.941	2.843	36.26	2.727	9.859	27.72	139.7
$\langle r_{+-}^2\rangle$	0.237	0.749	1.868	18.65	2.971	7.457	17.67	74.09
$\langle \delta(r_{--})\rangle$	0.65	0.26	0.15	0.15	0.019	0.0089	0.0051	0.0047
$\langle \delta(r_{++})\rangle$	0	0.0032	0.014	0.022	0	0.000029	0.00021	0.00032
$\langle \delta(r_{+-})\rangle$	2.0	1.2	0.87	0.73	0.17	0.11	0.076	0.068

the other particles with increasing σ, leading to an X_2+h two-cluster structure. (Both the energy and the equilibrium distance of the holes for H_3^+ are in good agreement with those obtained by adiabatic calculations.[23]) In fact, the *e-e* distance around the stability limit is close to that obtained for X_2 with $\sigma=\sigma_{\rm cr}$. This argument is further corroborated by the behavior of the correlation functions between the particles. Here the correlation function, $C(\mathbf{r})$, between particles i and j is defined by

$$C(\mathbf{r})=r^2\langle\Psi|\,\delta(\mathbf{r}_i-\mathbf{r}_j-\mathbf{r})|\Psi\rangle \tag{9}$$

for the 3D case and

$$C(\mathbf{r})=r\langle\Psi|\,\delta(\mathbf{r}_i-\mathbf{r}_j-\mathbf{r})|\Psi\rangle \tag{10}$$

for the 2D case. In Fig. 8 we show the correlation functions for three cases: For example, for the 2D X_3^+ system three cases include (a) $\sigma=0.01$, (b) $\sigma=0.15$, and (c) $\sigma=0.25$. Case (a) is near the hydrogenic limit, while case (c) is close to the stability limit. The correlation function for the holes depends on σ dramatically: It is sharply peaked near the hydrogenic limit corresponding to the triangular configuration with small variance but has a very wide distribution around the stability limit. In the stability limit the distribution has one peak reflecting the underlying X_2 subsystem as well as one plateau corresponding to the separated hole. On the contrary, the correlation function between the electrons changes rather moderately in three cases.

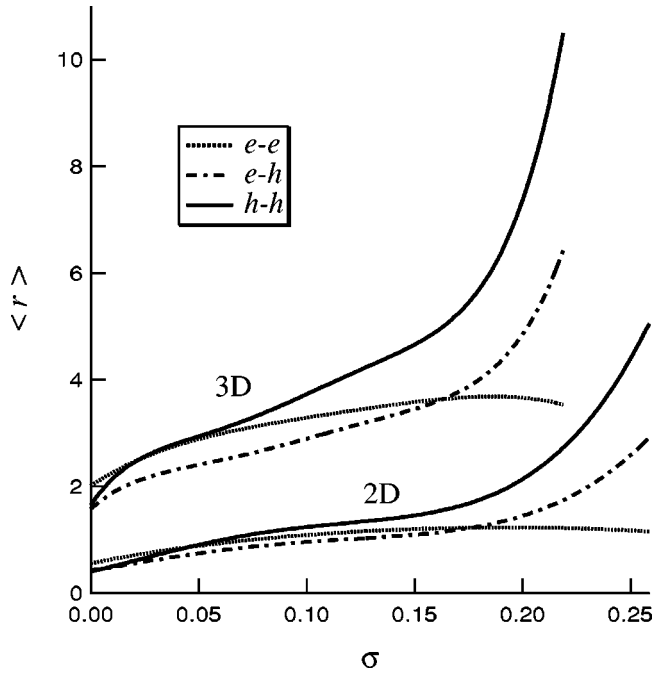

FIG. 7. The average distances of the constituents in the charged biexciton X_3^+ $(eehhh)$ as a function of the mass ratio σ. The length is in units of the excitonic Bohr radius.

D. Excited states of the biexciton

Most theoretical investigations have concentrated on the ground state of the biexciton. This system, however, has several excited states as well. The energies and properties of the excited states constitute very important information which may show the extent of the validity of the model with pure Coulomb interaction. The energy difference between the excited states and the ground state is a very characteristic property and different biexciton models would lead to different excitation energies.

In our previous paper[14] we have searched for bound excited states of the positronium molecule Ps_2. To this end, we have calculated the energies of different L (orbital angular momentum in 3D or its z component in the 2D case) and S (spin) states of Ps_2. We have not found any bound excited state below the Ps+Ps (atom-atom) threshold. There are states, however, for which the Ps+Ps channel is closed due to symmetry considerations,[15,24] and they can only decay into the Ps+Ps* (ground-state atom-excited-state atom) channel. We have found that a state with $(L,S)=(1,0)$ and negative parity is below the Ps+Ps* threshold, so that it forms a bound state. Another state, with quantum numbers $(L,S)=(0,1)$ and positive parity, is also below this threshold.[17,24]

We have calculated the energies of these two excited states as a function of the mass ratio. The details of the basis function for nonzero orbital angular momentum are given in Refs. 15 and 19. These states remain bound for any mass ratio in both 2D and in 3D (see Fig. 9). The electron spins are coupled to zero in both excited states, while two holes are in a spin-singlet state in the negative-parity excited state and

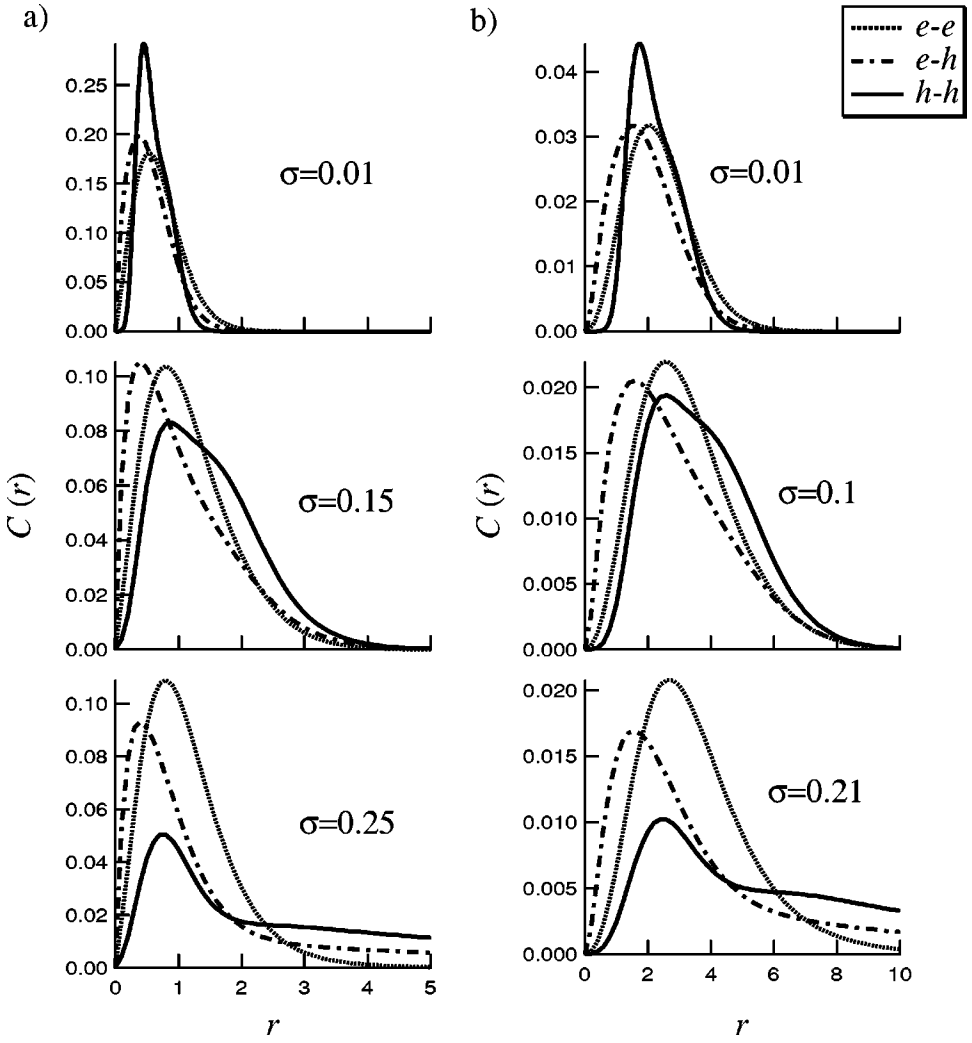

FIG. 8. The correlation functions for the charged biexciton $X_3^+(eehhh)$ for three typical values of the mass ration σ. (a) For 2D and (b) for 3D. The excitonic units are used.

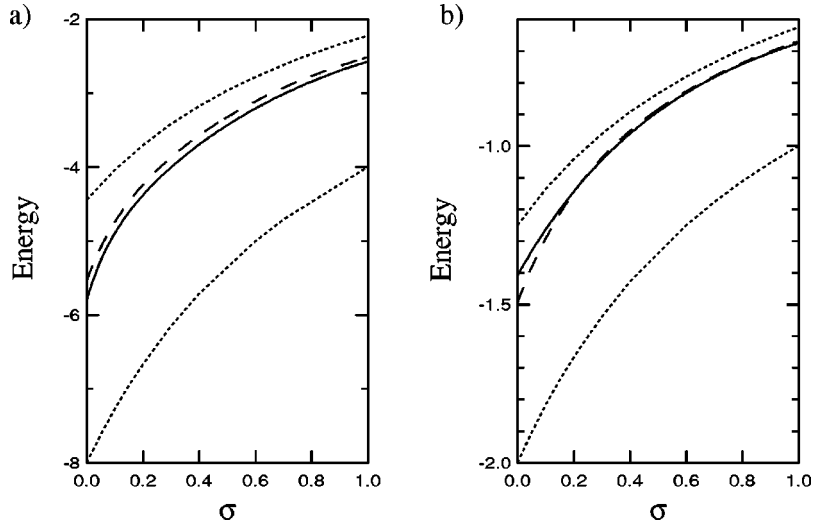

FIG. 9. The total energies of the excited states of the biexciton X_2 $(eehh)$ as a function of the mass ratio σ. (a) For 2D and (b) for 3D. The solid curves are the energies of the negative-parity state with $(L,S)=(1,0)$ and the dashed curves are the energies of the positive-parity state with $(L,S)=(0,1)$. The dotted curves are the threshold energies of $X+X$ and $X+X^*$, respectively. The energy is in units of the excitonic Rydberg.

in a spin-triplet state in the positive-parity excited state, respectively. To form a state with $(L,S)=(0,1)$, it is possible to couple the electrons to a spin-triplet state and the holes to a spin-singlet state. We have found that the state of this symmetry is also bound and that its energy is close to that of the positive-parity excited state mentioned above. The negative-parity state with $(L,S)=(1,0)$ may have more importance because it can be excited by an electric dipole transition.

IV. DISCUSSIONS

This work gives a unified numerical description of the excitonic complexes in 2D and 3D. We have investigated the excitonic trions, the biexcitons, and the charged biexcitons. The model we have considered here takes pure Coulomb interaction between the particles, neglecting the effect of all other circumstances, such as electronic bands, confinement, mirror charges, etc. Though this is certainly just an approximation to the realistic situation, hopefully this clear model case helps to understand the basic physics of these systems. Our variational approach is free of any bias and contains no approximation (i.e., we do not neglect the exchange interaction, etc.).

The novelty of this work is the investigation of the stability of the charged biexcitons. A very accurate calculation is required to find the stability domain. When the mass ratio approaches the border of the stable domain, the binding energy becomes very very tiny and the size of the system becomes extremely large. At the end of this process, the binding energy becomes zero (the size of the system in principle could become infinite at this point) and finally the charged biexciton autodissociates by ''emitting'' a hole. The critical mass ratio, where the charged biexciton becomes unbound, is around $\sigma_{cr}=0.22$ in 3D and $\sigma_{cr}=0.26$ in 2D. This means that the charged biexciton is not bound for any mass ratio but it has a stability domain $0\leqslant\sigma<\sigma_{cr}$.

The properties of the 2D and 3D systems are found to be generally very similar. Even though the binding energy and therefore the relative distances are very different in 2D and 3D, the binding energies and average distances, etc. show very similar behavior as a function of σ. It is a striking similarity that the stability of the charged biexciton is lost nearly exactly at the same σ_{cr} in 2D and 3D.

We have pointed out here that the excitonic complexes are highly nontrivial quantum-mechanical systems in both 2D and 3D. The relative motion of the particles is complicated and it is impossible to model these systems by some rigid geometrical picture, e.g., by assuming that the biexciton forms a static square in 2D. The interpretation of the biexciton molecule as a system of two exciton atoms is also oversimplified.

Besides the X_3^+ charged biexciton, we have tried to investigate the $X_2^-(hheee)$ system as well. In 3D, the $\sigma=0$ case would correspond to the H_2^-. In a fully adiabatic approach, if the distance between the two (infinitely heavy) protons is larger than 1.6 a.u., the potential energy curve of H_2^- is slightly below of that of H_2, indicating a bound system.[25] In the realistic situation where the proton mass is finite, this state is realized as a broad resonance.[26] In accordance with this, we have found no bound X_2^- for any σ value in both 2D and 3D. If either the X_2^- for any σ or the X_3^+ outside the $0\leqslant\sigma<\sigma_{cr}$ interval were found to be bound experimentally, that would indicate that other mechanisms play an important role in the binding.

Besides the ground state of the biexciton, we have also investigated the two excited states as well. Both states are above the exciton plus exciton threshold but their decay to that channel is forbidden. If a biexciton would be completely isolated, such excited states could remain bound. In the real experimental situation, however, they can interact in the surrounding material and they would decay. The first excited state that we studied belongs to $L=0$ and $S=1$. This state differs from the ground state by only its spin. Its experimental observation could be difficult and unlikely. The other excited state with $L=1$ and $S=0$ is more interesting. This system is practically formed by an exciton and an excited exciton atom. This state may be excited by an electric dipole transition from the ground state with a charasteristic photon energy so its experimental observation might be more realistic.

ACKNOWLEDGMENTS

This work was supported by Grants-in-Aid for Scientific Research (Nos. 08044065 and 10640255) of the Ministry of Education, Science and Culture (Japan) and OTKA Grant No. T17298 (Hungary). The work of K.V. was also supported by the U. S. Department of Energy, Nuclear Physics Division, under Contract No. W-31-109-ENG-39.

*Permanent address: Institute of Nuclear Research of the Hungarian Academy of Sciences (ATOMKI), Debrecen, H-4001, Hungary.

[1] R. C. Miller, D. A. Kleinman, A. C. Gossard, and O. Munteanu, Phys. Rev. B **25**, 6545 (1982).

[2] J. R. Haynes, Phys. Rev. Lett. **17**, 860 (1966).

[3] D. Birkedal, J. Singh, V. G. Lyssenko, J. Erland, and J. M. Hvam, Phys. Rev. Lett. **76**, 672 (1996).

[4] E. A. Hylleraas and A. Ore, Phys. Rev. **71**, 493 (1947).

[5] W. F. Brinkmann, T. M. Rice, and B. Bells, Phys. Rev. B **8**, 1570 (1973).

[6] D. A. Kleinman, Phys. Rev. B **28**, 871 (1983).

[7] B. Stebe and A. Ainane, Superlattices Microstruct. **5**, 545 (1989).

[8] Y. Kayanuma and K. Kuroda, Appl. Phys. A: Solids Surf. **53**, 475 (1991).

[9] T. Takagahara, Phys. Rev. B **39**, 10206 (1989).

[10] Al. L. Efros and A. V. Rodina, Solid State Commun. **72**, 645 (1989).

[11] C. Riva, F. M. Peeters, and K. Varga, Phys. Status Solidi B (to be published).

[12] K. Varga and Y. Suzuki, Phys. Rev. C **52**, 2885 (1995); Phys. Rev. A **53**, 1907 (1996).

[13] K. Varga and Y. Suzuki, Comput. Phys. Commun. **106**, 157 (1997).

[14] K. Varga, J. Usukura, and Y. Suzuki, Phys. Rev. Lett. **80**, 1876 (1998).

[15] J. Usukura, K. Varga, and Y. Suzuki, Phys. Rev. A **58**, 1918 (1998).
[16] W. Cencek and J. Rychlewski, J. Chem. Phys. **98**, 1252 (1993).
[17] D. B. Kinghorn and R. D. Poshusta, Phys. Rev. A **47**, 3671 (1993).
[18] P. M. Kozlowski and L. Adamowicz, Phys. Rev. A **48**, 1903 (1995); A. M. Frolov, S. I. Kryuchkov, and V. H. Smith, Jr., *ibid.* **51**, 4514 (1995).
[19] Y. Suzuki and K. Varga, *Stochastic Variational Approach to Quantum-Mechanical Few-Body Problems*, Lecture Notes in Physics Vol. m54 (Springer-Verlag, Berlin, 1998).
[20] A. Thilagam, Phys. Rev. B **55**, 7804 (1997).
[21] W. Cencek and W. Kutzelnigg, J. Chem. Phys. **105**, 5878 (1996).
[22] J. Singh, D. Birkedal, V. G. Lyssenko, and J. M. Hvam, Phys. Rev. B **53**, 15 909 (1996).
[23] R. Röhse, W. Klopper, and W. Kutzelnigg, J. Chem. Phys. **99**, 8830 (1993); R. Röhse, W. Kutzelnigg, R. Jaquet, and W. Klopper, *ibid.* **101**, 223 (1994).
[24] C. G. Bao, Phys. Lett. A **243**, 215 (1998).
[25] T. E. Sharp, At. Data **2**, 119 (1971).
[26] G. J. Shultz, Rev. Mod. Phys. **45**, 423 (1973).